Using the Outphasing Technique with Switching-Mode Power Converters for Visible Light Communication

Juan Rodríguez, Diego G. Lamar, Daniel G. Aller, Pablo F. Miaja and Javier Sebastián.
{rodriguezmjuan, gonzalezdiego, garciaadaniel, fernandezmiapablo, sebas}@uniovi.es.
Dpto. de Ingeniería Eléctrica, Electrónica, de Computadores y Sistemas. Grupo de Sistemas Electrónicos de Alimentación (SEA). Universidad de Oviedo. Edificio Departamental Oeste nº 3, Campus Universitario de Viesques. 33204 Gijón. España.

***Abstract*- A technique that provides variable output voltage from the output voltage ripple of a Switching-Mode Power Converter (SMPC) is explained in this work. The generated variable voltage is used to reproduce the communication signal of a Visible Light Communication (VLC) transmitter, thus avoiding the use of power inefficient Linear Power Amplifiers (LPAs). The proposed method uses the outphasing technique, which has been widely studied for switching-mode radiofrequency power amplifiers, with a SMPC that is responsible for both biasing the High-Brightness LEDs (HB-LEDs) and reproducing the communication signal.**

I. Introduction

Visible Light Communication (VLC) is a wireless communication system that uses the light intensity emitted by High-Brightness LED (HB-LED) bulbs (s(t)) not only for lighting, but also for transmitting information [1]. As a consequence, s(t) is made up of a DC component (s_{DC}) that establishes the lighting level, plus a high frequency AC component ($s_{AC}(t)$) that cannot be seen by a human eye and that is determined by the modulation scheme. In VLC, the HB-LED driver must be able to make use of all the bandwidth provided by the HB-LEDs (between 3 and 20 MHz depending on the HB-LED kind) to maximize the bit rate. In other words, the bandwidth of the driver should be higher than that of the HB-LEDs. Typically, a Switching-Mode Power Converter (SMPC) is used to drive the HB-LEDs in lighting applications because it achieves very high power efficiency (above 90%). However, conventional SMPCs are not fast enough to reproduce the communication signal component (i.e., $v_{O\text{-}AC}(t)$) and, consequently, the use of Linear Power Amplifiers (LPAs) has been adopted in order to reproduce that signal (see Fig. 1). Unfortunately, this approach leads to increase the energy consumption because a Class A or AB LPA offers very low power efficiency (between 10% and 40% depending on the modulation scheme) [2].

This work aims to explain a simple and power-efficient method to design a HB-LED driver for VLC. The approach is based on using the outphasing technique, which has been widely studied for switching-mode radiofrequency power amplifiers (class D, E and F) in order to reach a power-efficient amplifier able to reproduce amplitude-modulated signals [3]. In this work, the outphasing technique is used with a SMPC that is responsible for both biasing the HB-LEDs and reproducing the communication signal (see Fig. 1) [4].

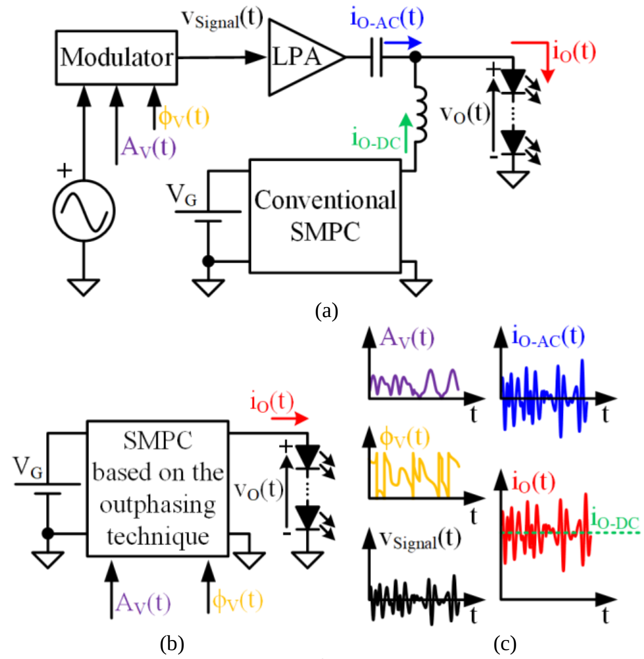

Fig. 1. (a) Driver based on the use of a LPA. (b) Proposed driver. (c) Main electrical waveforms.

II. Proposed HB-LED Driver for VLC

A. Requirements

In order to reproduce the communication signal, the driver must be able to provide the following voltage:

$$v_O(t) = v_{O-DC} + v_{O-AC}(t), \tag{1}$$

$$v_{O-AC}(t) = A_V(t)\cos(2\pi f_O t + \phi_V(t)), \tag{2}$$

where $v_{O\text{-}DC}$, $v_{O\text{-}AC}(t)$, $A_V(t)$, $\phi_V(t)$ and f_O are the DC component of $v_O(t)$, the AC component of $v_O(t)$, the amplitude modulation of the voltage, the phase modulation of the voltage and the center frequency of the modulation scheme, respectively. Hence, the HB-LED driver must be able to fulfill four requirements:

- Controlling $v_{O\text{-}DC}$ in order to ensure the desired lighting level.
- Generating a cosine waveform (carrier).
- Controlling the amplitude of the cosine waveform in order to perform the amplitude modulation (i.e., $A_V(t)$).
- Controlling the phase of the cosine waveform in order to perform the phase modulation (i.e., $\phi_V(t)$).

B. The Buck Converter

The buck converter is the fundamental SMPC. As Fig. 2 shows, it is based on generating a pulse voltage waveform ($v_S(t)$) by means of an input voltage (V_G) and two complementary switches. This voltage waveform is pulse-width modulated and, after that, it is filtered in order to control the output voltage (i.e., $v_O(t)$) through the width of the pulses. It implies that the cut-off frequency of the low-pass filter (f_C) must be much lower than the frequency of the pulse signal (f_S). Therefore, a variable output voltage can be generated by modulating the width of the pulses. In this case, the switching frequency of the transistors (i.e., f_S), must be around 20 times higher than the maximum frequency of the signal that is going to be reproduced. Unfortunately, this is not a suitable approach for driving the HB-LEDs of a VLC transmitter because the maximum frequency of the signal could reach the MHz range and, consequently, f_S becomes unaffordable since the switching losses of the SMPC would damage dramatically the power efficiency.

C. The SMPC based on the Outphasing Technique

The proposed SMPC meets the requirements indicated in Section II.A by using the output voltage ripple to reproduce the communication signal. The SMPC topology is a two-phase synchronous buck converter with high order output filter (see Fig. 3). However, since the communication signal is reproduced by means of the output voltage ripple, the output filter design differs from the conventional one of a SMPC. In this case the filter passes not only the DC component of both switch-node voltages ($v_{S\text{-}1}(t)$ and $v_{S\text{-}2}(t)$), but also their 1st switching harmonic. Hence, the cut-off frequency of the low-pass filter (f_C) must be between f_S and $2{\cdot}f_S$. As is explained below, the 1st switching harmonics of $v_{S\text{-}1}(t)$ and $v_{S\text{-}2}(t)$ will be used as the two phase-modulated carriers involved in the outphasing technique. Since these harmonics have the same amplitude and frequency, they can be phase-modulated and summed in order to obtain an amplitude-modulated and phase-modulated carrier.

Another major difference with respect to a conventional SMPC is that the proposed one is not controlled by applying the Pulse-Width Modulation (PWM) technique. It is controlled by using a more complex technique that has been called Pulse-Width and Pulse-Phase Modulation (PWPPM) in this paper. It implies that not only the width of the pulse is controlled, but also the position over the switching period (T_S). Fig. 4 shows an example of a pulse-width and pulse-phase modulated voltage. The duty cycle ($d(t)$) is the dimensionless parameter that is used to determine the width

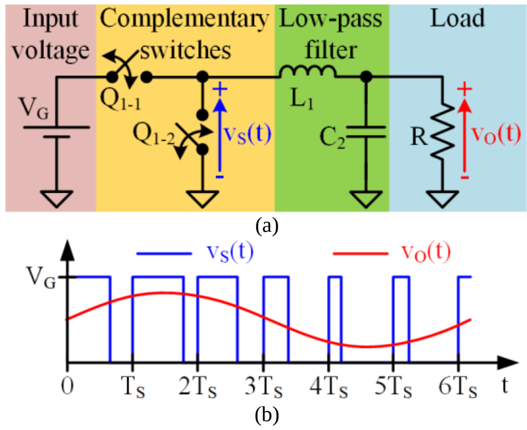

Fig. 2. Conventional buck converter: (a) Electrical circuit. (b) Main voltage waveforms.

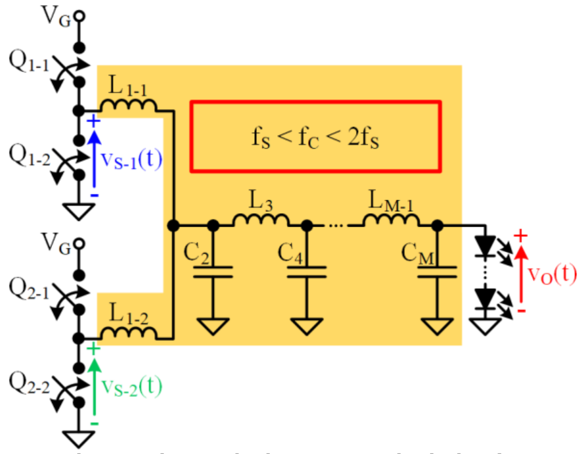

Fig. 3. Two-phase synchronous buck converter with a high order output filter that passes the DC component and the 1st switching harmonic of $v_{S\text{-}1}(t)$ and $v_{S\text{-}2}(t)$.

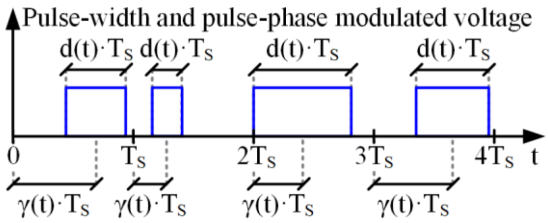

Fig. 4. Example of a pulse-width and pulse-phase modulated voltage.

of the pulses. It is important to note that controlling the phase of the pulses is equivalent to control their position. The dimensionless parameter that is used to control the phase of a pulse will be noted as $\gamma(t)$ (see Fig. 4), and it ranges between 0 and 1. When $\gamma(t)$ is 0, the pulse phase is 0 radians, and when $\gamma(t)$ is 1, the pulse phase is $-2{\cdot}\pi$ radians. Therefore, the pulse phase is equal to $-2{\cdot}\pi{\cdot}\gamma(t)$ radians and, consequently, the center of the pulse appears $T_S{\cdot}\gamma(t)$ seconds after the beginning of the switching period (see Fig. 4). Note that the phase is determined by the center of the pulse. As will be demonstrated later, the use of the PWPPM and the proposed filter design enable the reproduction of both $A_V(t)$ and $\phi_V(t)$. $d(t)$ is the same for both phases of the converter while the phases (i.e., the pulses positions) are modulated independently by means of $\gamma_1(t)$ and $\gamma_2(t)$. The equivalent circuits depicted in Fig. 5 will support the explanation of how $A_V(t)$ and $\phi_V(t)$ can be reproduced by controlling the phases (i.e., the positions) of $v_{S\text{-}1}(t)$ and $v_{S\text{-}2}(t)$. Since $v_{S\text{-}1}(t)$ and $v_{S\text{-}2}(t)$ are pulse voltage waveforms determined by the transistors states ($Q_{1\text{-}1}$ and $Q_{1\text{-}2}$ in the case of $v_{S\text{-}1}(t)$, and $Q_{2\text{-}1}$ and $Q_{2\text{-}2}$ in the case of $v_{S\text{-}2}(t)$), they can be considered as ideal pulse voltage sources (see Fig. 5(a)). The switch-node voltages can be expressed as a function of their harmonics by using the Fourier analysis:

$$v_{S-1}(t) = d(t)V_G + \sum_{k=1}^{\infty} \frac{2V_G}{k\pi} sin\big(k\pi d(t)\big)cos\big(k2\pi f_S t - k2\pi\gamma_1(t)\big), \tag{3}$$

$$v_{S-2}(t) = d(t)V_G + \sum_{k=1}^{\infty} \frac{2V_G}{k\pi} sin\big(k\pi d(t)\big)cos\big(k2\pi f_S t - k2\pi\gamma_2(t)\big). \tag{4}$$

The superposition theorem allows us to calculate $v_O(t)$ by analyzing the voltage contribution of each phase (see Fig. 5(b)):

$$v_O(t) = v_{O-1}(t) + v_{O-2}(t), \tag{5}$$

where $v_{O-1}(t)$ and $v_{O-2}(t)$ are the output voltages provided by phases 1 and 2, respectively. The circuit depicted in Fig. 5(c) can be obtained by considering that the phase inductors are equal and by applying the Thevenin's theorem. This circuit considers the switch-node voltage (i.e., $v_{S-i}(t)$) divided by two and applied to a low-pass filter, where the equivalent first inductor (L_1) is half the phase inductor (L_{1-i}). The voltage contribution of each phase can be calculated by taking into account that the filter passes not only the DC component, but also the 1st switching harmonic, the delay introduced by the filter (t_{Fil}) and (3)-(4):

$$v_{O-1}(t + t_{Fil}) = \frac{d(t)V_G}{2} + \frac{V_G}{\pi} sin\big(\pi d(t)\big)cos\big(2\pi f_S t - 2\pi\gamma_1(t)\big), \tag{6}$$

$$v_{O-2}(t + t_{Fil}) = \frac{d(t)V_G}{2} + \frac{V_G}{\pi} sin\big(\pi d(t)\big)cos\big(2\pi f_S t - 2\pi\gamma_2(t)\big). \tag{7}$$

Substituting (6)-(7) into (5) allows us to expresses $v_O(t)$ in the following way:

$$v_O(t + t_{Fil}) = d(t)V_G + \frac{2V_G}{\pi} sin\big(\pi d(t)\big)cos\big(\pi\alpha(t)\big)cos\big(2\pi f_S t - 2\pi\beta(t)\big). \tag{8}$$

where $\alpha(t)$ is the phase-shift between $v_{S-1}(t)$ and $v_{S-2}(t)$ (i.e., the position difference) divided by $2\cdot\pi$, and $\beta(t)$ is the absolute value of the mean phase of $v_{S-1}(t)$ and $v_{S-2}(t)$ (i.e., the average position) divided by $2\cdot\pi$ (i.e., the mean value of $\gamma_1(t)$ and $\gamma_2(t)$):

$$\alpha(t) = \gamma_2(t) - \gamma_1(t), \tag{9}$$

$$\beta(t) = \frac{\gamma_1(t) + \gamma_2(t)}{2}. \tag{10}$$

The identification of the amplitude modulation (i.e., $A_V(t)$) and the phase modulation (i.e., $\phi_V(t)$) of the voltage in (8) leads to the following expressions:

$$A_V(t) = \frac{2V_G}{\pi} sin\big(\pi d(t)\big)cos\big(\pi\alpha(t)\big), \tag{11}$$

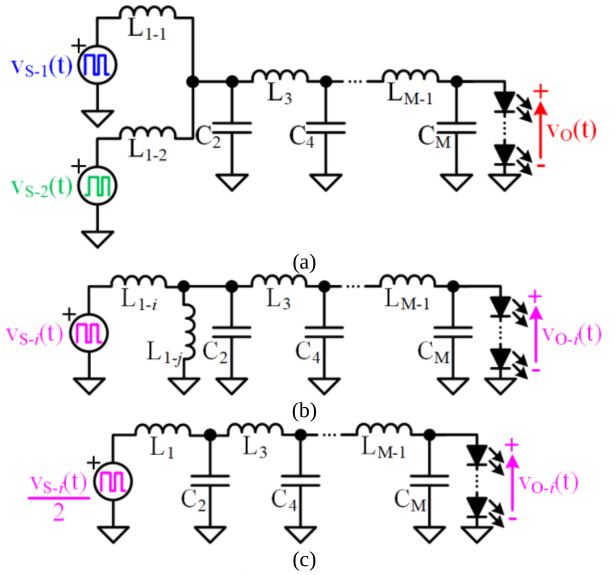

Fig. 5. Equivalent circuits of the proposed SMPC: (a) Considering the switch-node voltages as ideal pulse voltage sources. (b) Applying the superposition theorem to calculate voltage contribution of phase *i*. (c) Applying the Thevenin's theorem to calculate voltage contribution of phase *i*.

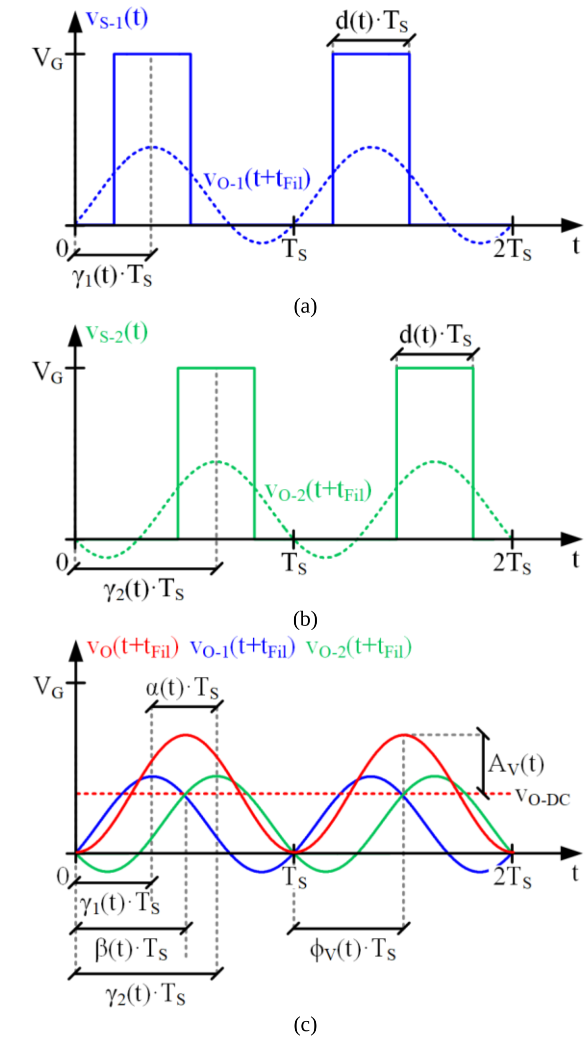

Fig. 6. Main voltage waveforms of the proposed SMPC: (a)-(b) Switch-node voltages. (c) Output voltage.

$$\phi_V(t) = -2\pi\beta(t). \tag{12}$$

According to (11), $\alpha(t)$ can be used to control $A_V(t)$. It is stablished that $\alpha(t)$ must range between 0 and 0.5 limits. Note that an $\alpha(t)$ value higher that 0.5 leads to a sign change and, consequently, to a phase modification. When $\alpha(t)$ is 0 (i.e., the phase-shift is 0 radians), the maximum amplitude is reached. On the other hand, when $\alpha(t)$ is 0.5 (i.e., the phase-shift is π radians), the amplitude is 0 V. According to (12), $\beta(t)$ can be used to control $\phi_V(t)$. $\beta(t)$ ranges between 0 and 1. When $\beta(t)$ is 0, $\phi_V(t)$ is 0 radians; and when $\beta(t)$ is 1, $\phi_V(t)$ is $-2\cdot\pi$ radians. Fig. 6 shows the main voltage waveforms involved in the process and the control parameters. In order to exemplify the operation of the proposed SMPC, Fig. 7 considers different d(t), $\alpha(t)$ and $\beta(t)$ values that are indicated in Table I. In Fig. 7(b), a decrease of $A_V(t)$ is performed by increasing $\alpha(t)$. $\phi_V(t)$ is decreased in Fig. 7(c) by increasing $\beta(t)$. Finally, $v_{O\text{-}DC}$ is increased in Fig. 7(d) by increasing d(t). Note that in the last case, since d(t) also affects $A_V(t)$ (see (11)), $\alpha(t)$ must be recalculated to not modify $A_V(t)$.

III. Experimental Results

A two-phase synchronous buck converter with 10th order Butterworth filter was built in order to validate the proposed HB-LED driver for VLC. The cut-off frequency of the filter is 650 kHz ($L_{1\text{-}1}$=$L_{1\text{-}2}$=4.26 µH, C_2=82 nF, L_3=2.47 µH, C_4=74 nF, L_5=2.05 µH, C_6=57 nF, L_7=1.42 µH, C_8=34 nF, L_9=633 nH and C_{10}=7 nF). The SMPC supplies a string of five HB-LEDs (W42180 Seoul Semiconductor). The switching frequency is 500 kHz, the input voltage is 30 V and the maximum power is around 10 W. The power efficiency of the proposed SMPC ranges between 95% and 96.5% depending on the dimming level. Fig. 8 shows the main experimental waveforms of the SMPC in steady-state conditions (i.e., constant $A_V(t)$ and $\phi_V(t)$). As can be seen, the cosine waveform is reproduced with high accuracy. In order to evaluate the capability to reproduce a communication signal, a multi-carrier modulation scheme that is made up of six carriers (c_1, c_2, …, c_6) was reproduced. The commercial receiver PDA10A-EC provides a voltage waveform ($v_{RX}(t)$) that is proportional to the received light intensity. Fig. 9(a) shows the main waveforms of the VLC setup in the time domain when the aforementioned MCM scheme is reproduced. Moreover, Fig. 9(b) shows the magnitude of $v_{RX}(t)$ in the frequency domain.

IV. Conclusions

The proposed SMPC based on the outphasing technique is a very interesting approach for the HB-LED drivers of VLC transmitters. It achieves high power efficiency because of the use of a SMPC, thus avoiding the use of power inefficient LPAs. Moreover, the power stage is simpler and the required f_S is much lower than in the case of conventional pulse-width modulated SMPCs, which facilitates the practical implementation and leads to lower switching losses (main source of losses in this application).

Acknowledgements

This work has been supported by the Spanish Government under the Project MINECO-17-DPI2016-75760-R, the Principality of Asturias under the Project IDI/2018/000179, the grant BP17-91 and by European Regional Development Fund (ERDF) grants.

References

[1] S. Dimitrov, and H. Haas, *Principles of LED light communications. Towards networked Li-Fi*. Cambridge University Press, 2015.

[2] J. Sebastián, D. G. Lamar, D. G. Aller, J. Rodríguez and P. F. Miaja, "On the role of power electronics in visible light communication," in IEEE Journal of Emerging and Selected Topics in Power Electronics, vol. 6, no. 3, pp. 1210-1223, Sept. 2018.

[3] D. Cox, "Linear Amplification with Nonlinear Components," in IEEE Transactions on Communications, vol. 22, no. 12, pp. 1942-1945, December 1974.

[4] J. Rodríguez, D. G. Lamar, P. F. Miaja and J. Sebastián, "Reproducing single-carrier digital modulation schemes for VLC by controlling the first switching harmonic of the DC–DC power converter output voltage ripple," in IEEE Transactions on Power Electronics, vol. 33, no. 9, pp. 7994-8010, Sept. 2018.

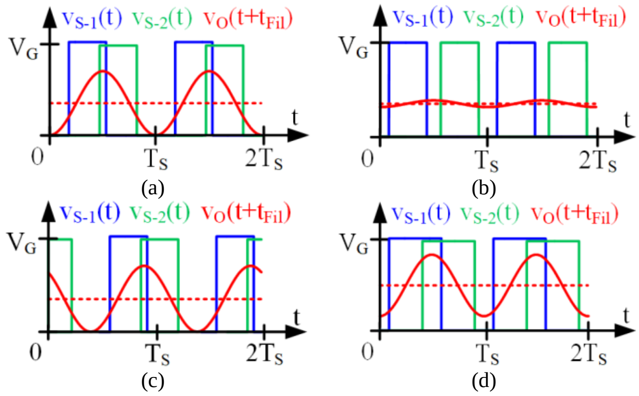

Fig. 7. Four examples of pulses situations: (a) Initial conditions. (b) Decrease of $A_V(t)$. (c) Decrease of $\phi_V(t)$. (d) Increase of $v_{O\text{-}DC}$.

TABLE I
MAIN PARAMETERS OF THE OPERATION EXAMPLE DEPICTED IN FIG. 7

	d(t)	α(t)	β(t)	$v_{O\text{-}DC}$	$A_V(t)$	$\phi_V(t)$
Example 1	0.35	0.29	0.5	$0.35\cdot V_G$	$0.35\cdot V_G$	$-\pi$
Example 2	0.35	0.48	0.5	$0.35\cdot V_G$	$0.04\cdot V_G$	$-\pi$
Example 3	0.35	0.29	0.9	$0.35\cdot V_G$	$0.35\cdot V_G$	$-1.8\cdot\pi$
Example 4	0.5	0.32	0.5	$0.5\cdot V_G$	$0.35\cdot V_G$	$-\pi$

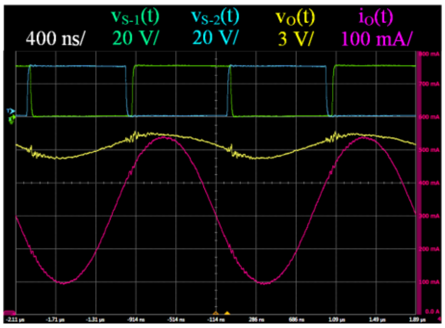

Fig. 8. Main experimental waveforms of the HB-LED driver for VLC in steady-state conditions.

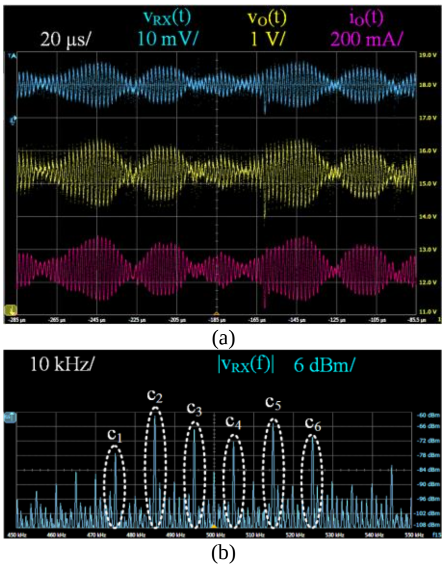

Fig. 9. Main experimental waveforms of the VLC link (distance: 40 cm): (a) Time domain. (b) Frequency domain.